CHAPTER - 02

VIBRATION ANALYSIS OF ELECTRO-MAGNETO TRANSVERSELY ISOTROPIC NON-LOCAL THERMOELASTIC CYLINDER WITH VOIDS

2.1 Introduction

In this chapter the free vibrations of transversely isotropic nonlocal electro-magneto thermoelastic hollow cylinder with voids have been addressed in the preview of generalized thermoelasticity. The governing equations and the constitutive relations are transformed into coupled ordinary differential equations by applying time harmonic variations. The boundary conditions of the outer and the inner surfaces of the hollow cylinder are considered to be traction free, no change in voids volume fraction and thermally insulated/isothermal temperature field. The analytical results for frequency equations are presented and validated with existing literature. To explore the free vibration analysis from the considered boundary conditions, the numerical Iteration method has been applied to create data by using MATLAB software tool. The obtained analytical results are represented graphically with the assistance of numerical computations and simulations in absence/presence of magnetic field for nonlocal/local thermoelastic materials. To verify the elastic nonlocal effects in different models of thermoelasticity, the field functions are represented graphically with and without magnetic field effects.

2.2 Formulation of mathematical model

The nonlocal transversely isotropic magneto-thermoelastic hollow cylinder with voids of inner radius $R_I = a$ and outer radius $R_O = a\eta$ having domain $a \le r \le a\eta$, free from internal and external mechanical/thermal loads, initially at uniform temperature T_0 is shown in Fig. 2.1. The strength of magnetic field $\boldsymbol{H}$ proceeds in the direction of z-axis. Field components of cylinder with coordinates (r, θ, z) are assumed as displacement vector $\boldsymbol{u} = (u_r, u_\theta, u_z)$ where $u_r = u(r,t), u_\theta = 0, u_z = 0$, concentration of voids volume fraction $\varphi = \varphi(r,t)$ and temperature component $T = T(r,t)$. The strain vector i.e. dilatation $\boldsymbol{e} = \boldsymbol{e}_{rr} + e_{\theta\theta}$ has the strain components

$e_{rr} = \frac{\partial u}{\partial r}, e_{\theta\theta} = \frac{u}{r}, e_{zz} = 0,\ e_{r\theta} = 0 = e_{rz} = e_{\theta z}$. The Maxwell's equations have been generated by electro-magnetic field in the absence of charge density and displacement current as (Das et al. (2013))

$$\nabla \times \boldsymbol{E} = -\frac{\partial \boldsymbol{B}}{\partial t}, \quad \nabla \times \boldsymbol{H} = \boldsymbol{J}, \quad \boldsymbol{B} = \mu_e \boldsymbol{H}, \quad \nabla \cdot \boldsymbol{B} = 0. \tag{2.1}$$

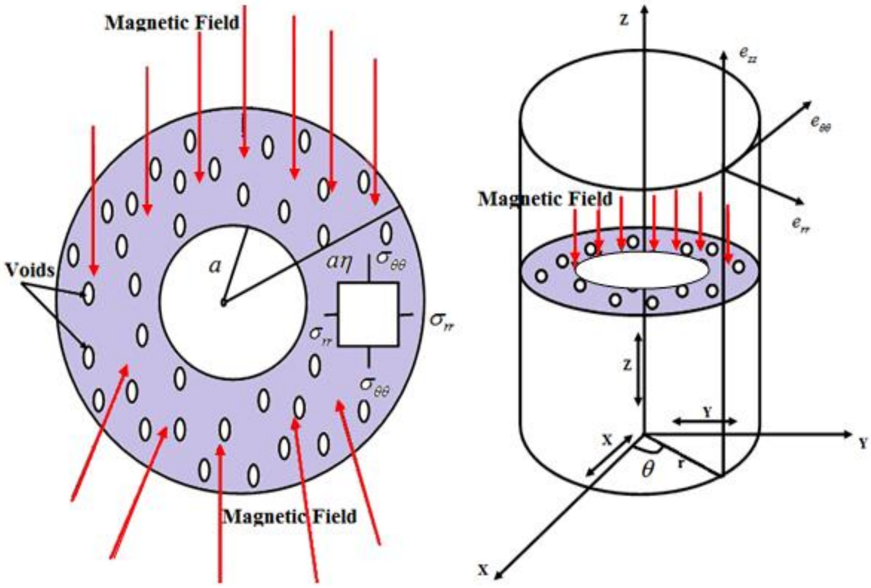

Figure 2.1: Geometry of the problem

In continua of deformation, the generalized Ohm's law is

$$\boldsymbol{J} = \sigma(\boldsymbol{E} + \frac{\partial u}{\partial t} \times \boldsymbol{B}). \tag{2.2}$$

Here $\boldsymbol{B}$ is the magnetic field, $\boldsymbol{J}$ is the current density which is neglected due to small influence of temperature gradient, $\boldsymbol{H} = \boldsymbol{H}_0 + \boldsymbol{h}$ is the strength of magnetic field, where $\boldsymbol{H}_0 = (0, 0, H_0)$, $\boldsymbol{h}$ is the perturbation of magnetic field which is so small that their product might be neglected due to linearization of the basic equations. Therefore, the basic governing equation of motion under the impact of electro magneto field, constitutive relations, equation of voids volume fraction and heat conduction equation without body forces, free from voids equilibrated forces and without heat sources are given as (Cowin and Nunziato (1983) and Dhaliwal and Singh (1980))

$$(1 - \zeta^2 \nabla^2)\sigma_{ij} = \sigma_{ij}^L \ \ (i, j = r, \theta). \tag{2.3}$$

Here the quantities having superscript $"L"$ stands for the local medium.

$$\left.\begin{aligned}(1-\zeta^2\nabla^2)\sigma_{rr} &= c_{11}\frac{\partial u}{\partial r}+c_{12}\frac{u}{r}+b\varphi-\beta_r T\\ (1-\zeta^2\nabla^2)\sigma_{\theta\theta} &= c_{12}\frac{\partial u}{\partial r}+c_{11}\frac{u}{r}+b\varphi-\beta_\theta T\end{aligned}\right\}. \tag{2.4}$$

Here $\zeta = e_0 a_0$ is the elastic nonlocal parameter, a_0 is the internal characteristic length and e_0 is a material constant, $\sigma_{rr}, \sigma_{\theta\theta}$ are the radial and circular stress components, $T=\theta-T_0$ is the change in temperature, T_0 is the temperature of the medium in its natural state assumed to be such that $|T/T_0| << 1$, θ is the absolute temperature, β_r, β_θ are the thermal modulii, where $\beta_r=\beta_\theta=(c_{11}+c_{12})\alpha_1+c_{13}\alpha_3$; $\alpha_1=\alpha_3=\alpha_T$ is the coefficient of linear thermal expansion (Dhaliwal and Singh (1980)), b is a void parameter, c_{11}, c_{12} are elastic constants whose values are as given below

$$c_{11}=\frac{E(1-\nu)}{(1+\nu)(1-2\nu)}\ ,\ \ c_{12}=\frac{E\nu}{(1+\nu)(1-2\nu)}=c_{13},$$

where ν is the Poisson ratio and E is the Young's modulus, $\nabla^2=\frac{\partial^2}{\partial r^2}+\frac{1}{r}\frac{\partial}{\partial r}$ is the Laplacian operator.

$$\frac{\partial\sigma_{rr}}{\partial r}+\frac{(\sigma_{rr}-\sigma_{\theta\theta})}{r}+\boldsymbol{F}_r=\rho(1-\zeta^2\nabla^2)\frac{\partial^2 u}{\partial t^2}, \tag{2.5}$$

where $\boldsymbol{F}_r$ is the component of body force $\boldsymbol{F}=(\boldsymbol{J}\times\boldsymbol{B})$ and ρ is the mass density.

$$\alpha\nabla^2\varphi-\left(\xi_1+\xi_2\frac{\partial}{\partial t}\right)\varphi-be+MT=\rho\chi(1-\zeta^2\nabla^2)\frac{\partial^2\varphi}{\partial t^2}, \tag{2.6}$$

where α, b are the void parameters, φ is corresponding to change in voids volume fraction field, χ is the equilibrated inertia, due to presence of voids ξ_1, ξ_2 are the material constants, M is thermo-void coupling parameter, e is the cubical dilatation.

$$\left(\frac{\partial}{\partial t}+t_0\frac{\partial^2}{\partial t^2}\right)\left(T_0\left(\beta_r\frac{\partial u}{\partial r}+\beta_\theta\frac{u}{r}\right)+MT_0\varphi\right)= \\ -\left(\frac{\partial}{\partial t}+t_0\frac{\partial^2}{\partial t^2}\right)\rho C_e T+\frac{1}{r}\frac{\partial}{\partial r}\left(rK\frac{\partial T}{\partial r}\right), \tag{2.7}$$

where C_e is specific heat at constant strain, t_0 is the relaxation time parameter which represent LS theory, K is the thermal conductivity.

2.3 Initial and boundary conditions

The transversely isotropic nonlocal magneto-thermoelastic hollow cylinder with voids is taken to be at undisturbed state and rest position initially, thermally as well as mechanically so that initial conditions take the forms:

$$u(r,0)=\varphi(r,0)=T(r,0)=0, \\ \frac{\partial u(r,0)}{\partial t}=\frac{\partial\varphi(r,0)}{\partial t}=\frac{\partial T(r,0)}{\partial t}=0 \quad \text{at} \quad r=a\ ,\ a\eta \tag{2.8}$$

The boundary conditions are assumed as follows:

Set I:

$$\sigma_{rr}=0\ ,\ \varphi=0\ ,\ \frac{\partial T}{\partial r}=0 \quad \text{at} \quad r=a\ ,\ r=a\eta. \tag{2.9}$$

Set II:

$$\sigma_{rr}=0\ ,\ \varphi=0\ ,\ T=0 \quad \text{at} \quad r=a\ ,\ r=a\eta. \tag{2.10}$$

2.4 Solution of the problem

Now first part of equation (2.1) yields

$$\frac{\partial H_r}{\partial t}=0\ , \quad \frac{\partial H_\theta}{\partial t}=\frac{1}{\mu_e}\frac{\partial E_z}{\partial r}\ , \quad \frac{\partial H_z}{\partial t}=-\frac{1}{\mu_e}\frac{\partial}{\partial r}(rE_\theta). \tag{2.11}$$

The second part of equation (2.1) gives

$$J_r=0\ ,\ J_\theta=-\frac{\partial H_z}{\partial r}\ ,\quad J_z=\frac{1}{r}\frac{\partial}{\partial r}(rH_\theta), \tag{2.12}$$

where $\boldsymbol{H}=(H_r,H_\theta,H_z)$, $\boldsymbol{E}=(E_r,\mathrm{E}_\theta,\mathrm{E}_z)$ and $\boldsymbol{J}=(J_r,J_\theta,J_z)$.

The third part of equation (2.1) yields that in radial direction, no perturbed field is applied initially i.e. $\frac{\partial h_r}{\partial r} = 0$ which implies that $h_r = 0$.

From equation (2.2) the modified Ohm's law yields

$$J_r = \sigma E_r \ , \quad J_\theta = \sigma\left(E_\theta - \mu_e H_z \frac{\partial u}{\partial t}\right) \ , \quad J_z = \sigma\left(E_z - \mu_e H_\theta \frac{\partial u}{\partial t}\right). \tag{2.13}$$

From equation (2.11) as $J_r = 0$, which implies that $E_r = 0$.

To eliminate J_r, J_θ, J_z and using equations (2.1–2.2) and (2.13), we obtain

$$\left.\begin{aligned} \frac{\partial H_\theta}{\partial t} &= \frac{1}{(\sigma\mu_e)}\frac{\partial}{\partial r}\left(\frac{1}{r}\frac{\partial}{\partial r}(rH_\theta)\right) - \frac{\partial}{\partial r}\left(H_\theta \frac{\partial u}{\partial t}\right) \\ \frac{\partial H_z}{\partial t} &= \frac{1}{(\sigma\mu_e)}\left(\frac{1}{r}\frac{\partial H_z}{\partial r} + \frac{\partial^2 H_z}{\partial r^2}\right) - \frac{1}{r}\left(H_z \frac{\partial u}{\partial t}\right) - \frac{\partial}{\partial r}\left(H_z \frac{\partial u}{\partial t}\right) \end{aligned}\right\}. \tag{2.14}$$

Here $(\sigma\mu_e)^{-1}$ is magnetic viscosity. In setting the term $\boldsymbol{H} = H_0 + h$, the perturbation of magnetic field h is small in comparison with strong initial magnetic field H_0, the equation (2.14) can be written as

$$\left.\begin{aligned} \frac{\partial H_\theta}{\partial t} &= \frac{1}{(\sigma\mu_e)}\frac{\partial}{\partial r}\left(\frac{\partial h_\theta}{\partial r} + \frac{h_\theta}{r}\right) \\ \frac{\partial H_z}{\partial t} &= \frac{1}{(\sigma\mu_e)}\left(\frac{1}{r}\frac{\partial h_z}{\partial r} + \frac{\partial^2 h_z}{\partial r^2}\right) - H_0 \frac{\partial}{\partial t}\left(\frac{\partial u}{\partial r} + \frac{u}{r}\right) \end{aligned}\right\}. \tag{2.15}$$

The second part of equation (2.15) yields $h_z = -H_0\left(\frac{\partial u}{\partial r} + \frac{u}{r}\right)$ due to perfect electrical conductor, the magnetic viscosity $(1/\sigma\mu_e) \to 0$ as $\sigma \to \infty$, hence no perturbation has been observed at ∞. Therefore, the equation (2.5) reduces to

$$\frac{\partial \sigma_{rr}}{\partial r} + \frac{(\sigma_{rr} - \sigma_{\theta\theta})}{r} + \mu_e H_0^2 \frac{\partial}{\partial r}\left(\frac{\partial u}{\partial r} + \frac{u}{r}\right) = \rho(1 - \zeta^2\nabla^2)\frac{\partial^2 u}{\partial t^2}. \tag{2.16}$$

Substituting constitutive relations form equation (2.4) in equation (2.16) we obtain

$$\left(1 + \frac{\mu_e H_0^2}{c_{11}}\right)\left(\frac{\partial^2 u}{\partial r^2} + \frac{1}{r}\frac{\partial u}{\partial r} - \frac{u}{r^2}\right) + \frac{b}{c_{11}}\frac{\partial \varphi}{\partial r} - \frac{\beta_r}{c_{11}}\frac{\partial T}{\partial r} = \frac{\rho}{c_{11}}(1 - \zeta^2\nabla^2)\frac{\partial^2 u}{\partial t^2}. \tag{2.17}$$

Applying divergence to equation (2.17) we get

$$R_h\nabla^2 e+\frac{b}{c_{11}}\nabla^2\varphi-\frac{\beta_r}{c_{11}}\nabla^2 T=\frac{\rho}{c_{11}}(1-\zeta^2\nabla^2)\frac{\partial^2 e}{\partial t^2}, \tag{2.18}$$

where $R_h=1+\frac{\mu_e H_0^2}{c_{11}}$, $e=\frac{\partial u}{\partial r}+\frac{u}{r}$.

We set up following non-dimensional parameters to remove the complexity of above equations

$$\left.\begin{array}{l}(U\,,\,x,\,\zeta_0)=\frac{1}{a}(u,\,r\,,\,\zeta)\,,(\tau\,,\tau_0)=\frac{c}{a}(t,\,t_0),\,(\tau_{xx}\,,\,\tau_{\theta\theta})=\frac{1}{c_{11}}(\sigma_{rr},\,\sigma_{\theta\theta})\,,\\ \Theta=\frac{T}{T_0},c_0=\frac{c_{12}}{c_{11}},\\ c=\sqrt{\frac{c_{11}}{\rho}},\quad \phi=\frac{\chi\Omega^{*2}}{a^2}\varphi,\quad \bar{\xi}=\frac{c}{a}\frac{\xi_2}{\xi_1},\quad \bar{\beta}_R=\frac{\beta_r T_0}{c_{11}},\quad \bar{\beta}_\theta=\frac{\beta_\theta T_0}{c_{11}},\\ \bar{b}^*=\frac{a^2\bar{b}}{\chi\Omega^{*2}},\quad \bar{b}=\frac{b}{c_{11}}\end{array}\right\}. \tag{2.19}$$

Using non-dimensional parameters from equation (2.19) in equations (2.4), (2.6), (2.7) and (2.18), the non-dimensional form of equation have been obtained

$$\left.\begin{array}{l}(1-\zeta_0{}^2\nabla_x^2)\tau_{xx}=\frac{\partial U}{\partial x}+c_0\frac{U}{x}+\bar{b}^*\phi-\bar{\beta}_R\Theta\\ (1-\zeta_0{}^2\nabla_x^2)\tau_{\theta\theta}=c_0\frac{\partial U}{\partial x}+\frac{U}{x}+\bar{b}^*\phi-\bar{\beta}_\theta\Theta\end{array}\right\}, \tag{2.20}$$

$$R_h\nabla_x^2 e+\bar{b}^*\nabla_x^2\phi-\bar{\beta}_R\nabla_x^2\Theta=(1-\zeta_0^2\nabla_x^2)\frac{\partial^2 e}{\partial\tau^2}, \tag{2.21}$$

$$\nabla_x^2\phi-a_1\left(1+\bar{\xi}\frac{\partial}{\partial\tau}\right)\phi-a_2 e+a_3\Theta=\frac{1}{\delta_1^2}(1-\zeta_0^2\nabla_x^2)\frac{\partial^2\phi}{\partial\tau^2}, \tag{2.22}$$

$$\nabla_x^2\Theta-\Omega^*\left(\frac{\partial}{\partial\tau}+\tau_0\frac{\partial^2}{\partial\tau^2}\right)\Theta=\left(\frac{\partial}{\partial\tau}+\tau_0\frac{\partial^2}{\partial\tau^2}\right)(a_4 e+a_5\phi)\,,0 \tag{2.23}$$

where

$$a_1=\frac{\xi_1 a^2}{\alpha},a_2=\frac{b\chi\Omega^{*2}}{\alpha},a_3=\frac{M\chi\Omega^{*2}T_0}{\alpha},a_4=\frac{\varepsilon_T\,\Omega^*}{\bar{\beta}_R},a_5=\frac{cMa^3}{K\chi\Omega^{*2}},$$

$$\omega^* = \frac{c_{11}C_e}{K},\ \Omega^* = \frac{a\omega^*}{c},\ \ \varepsilon_T = \frac{T_0\beta_r^2}{\rho C_e c_{11}},\ \delta_1^2 = \frac{\alpha}{\chi c_{11}},\ \ \nabla_x^2 = \frac{1}{x}\frac{\partial}{\partial x}\left(x\frac{\partial}{\partial x}\right).$$

We introduce time harmonics vibrations from Pierce (1981):

$$\left(e,\ \phi,\ \Theta\right) = \left(\bar{e},\ \bar{\phi}\ ,\ \bar{\Theta}\right)e^{i\Omega\tau}, \tag{2.24}$$

where $\Omega = \dfrac{\omega a}{c}$ is the circular frequency.

Using (2.24) in equations (2.20–2.23), we get

$$\begin{pmatrix}\tau_{xx}\\ \tau_{\theta\theta}\end{pmatrix} = \begin{pmatrix}1 & \dfrac{c_0-1}{x} & \bar{b}^* & -\bar{\beta}_R \\ 1 & (c_0-1)\dfrac{\partial}{\partial x} & \bar{b}^* & -\bar{\beta}_\theta\end{pmatrix}\begin{pmatrix}\bar{e}\\ \bar{U}\\ \bar{\phi}\\ \bar{\Theta}\end{pmatrix}, \tag{2.25}$$

$$\left.\begin{array}{l}(\nabla_x^2 + A_{11})\ \bar{e} + A_{12}\nabla_x^2\bar{\phi} - A_{13}\nabla_x^2\bar{\Theta} = 0\\ -A_{21}\bar{e} + (\nabla_x^2 + A_{22})\ \bar{\phi} + A_{23}\bar{\Theta} = 0\\ A_{31}\bar{e} +\ A_{32}\bar{\phi} - (\nabla_x^2 - A_{33})\ \bar{\Theta} = 0\end{array}\right\}, \tag{2.26}$$

where $A_{11} = \dfrac{\Omega^2}{R_h - \zeta_0^2\Omega^2}, A_{12} = \dfrac{\bar{b}^*}{R_h - \zeta_0^2\Omega^2}, A_{13} = \dfrac{\bar{\beta}_R}{R_h - \zeta_0^2\Omega^2},$

$$A_{21} = \frac{a_2}{a_1^*},\ \ A_{22} = \frac{a_2^*}{a_1^*},\ \ A_{23} = \frac{a_3}{a_1^*}\ ,\ a_1^* = \frac{\delta_1^2 - \zeta_0^2\Omega^2}{\delta_1^2}\ ,\ a_2^* = \frac{a_1 i\Omega\bar{\xi}^*\delta_1^2 + \Omega^2}{\delta_1^2},$$

$$A_{31} = \Omega^2\tau_0^* a_4\ ,\ A_{32} = \tau_0^*\Omega^2 a_5\ ,\ \ A_{33} = \Omega^*\Omega^2\tau_0^*\ ,\ \ \tau_0^* = i\Omega^{-1} - \tau_0\ ,\ \bar{\xi}^* = i\Omega^{-1} - \bar{\xi}\ .$$

In order to obtain non-trivial solution for the unknown parameters $\bar{e},\ \bar{\phi}\ ,\bar{\Theta}$ in equation (2.26), the determinant of the coefficient matrix in equation (2.26) vanishes which leads to the following equation:

$$(\nabla_x^6 - L^*\nabla_x^4 + M^*\nabla_x^2 - N^*)(\bar{e}\ ,\ \bar{\phi},\ \bar{\Theta}) = 0, \tag{2.27}$$

where $L^* = (A_{33} - A_{11} - A_{22} - A_{12}A_{21} + A_{13}A_{31})$,

$$M^* = (A_{23}A_{32} - A_{22}A_{33} - A_{11}A_{33} + A_{11}A_{22} - A_{12}A_{21}A_{33} \\ -A_{12}A_{23}A_{31} - A_{13}A_{21}A_{32} - A_{13}A_{31}A_{22}),$$

$$N^* = (A_{11}A_{22}A_{33} - A_{11}A_{23}A_{33})\ .$$

This is to be analyzed that the solution of equation (2.27) which is bounded for $x \to \infty$, for this there is a requirement of the roots with positive real parts i.e. $\mathrm{Re}(k_i) \geq 0,\ \forall\ i = 1, 2, 3)$. Therefore, roots $k_i;\ i = 1, 2, 3$ of equation (2.27) have been achieved as given below:

$$k_1 = \sqrt{\frac{1}{3}\left(2A\sin B + L^*\right)},\ k_2 = \sqrt{\frac{1}{3}\left(L^* - A(\sqrt{3}\cos B + \sin B)\right)},$$
$$k_3 = \sqrt{\frac{1}{3}\left(L^* + A(\sqrt{3}\cos B - \sin B)\right)},$$

where, $A = \sqrt{L^{*2} - 3M^*},\ C = -\dfrac{2L^{*3} - 9L^*M^* + 27N^*}{2L^{*3}},\ B = \dfrac{1}{3}\sin^{-1}(C)$.

Consequently, the complete solution of equation (2.27) might be written as

$$\bar{\Theta} = \sum_{i=1}^{3}\left[P_i J_0(k_i x) + Q_i Y_0(k_i x)\right], \tag{2.28}$$

$$\bar{e} = \sum_{i=1}^{3} R_i\left[P_i J_0(k_i x) + Q_i Y_0(k_i x)\right], \tag{2.29}$$

$$\bar{\phi} = \sum_{i=1}^{3} S_i\left[P_i J_0(k_i x) + Q_i Y_0(k_i x)\right], \tag{2.30}$$

where, $R_i = \dfrac{k_i^4(A_{13} - A_{12}A_{23}) + k_i^2 A_{13}A_{22}}{k_i^4 + (A_{11} + A_{22} + A_{12}A_{21})k_i^2 + A_{11}A_{22}}$, $S_i = -\dfrac{k_i^2(A_{23}A_{31} - A_{21}) + A_{21}A_{33}}{k_i^2 A_{31} + A_{22}A_{31} + A_{21}A_{32}}$.

Here $P_i, Q_i;\ (i = 1, 2, 3)$ are constants that depend on Ω only. Here J_0 and Y_0 are modified Bessel functions of order zero with First and Second kinds only. Resolving cubical dilation $(\bar{e})$ from equation (2.29) for displacement $\bar{U}$, we obtain

$$\bar{U} = \sum_{i=1}^{3}\frac{1}{k_i} R_i\left(P_i J_1(k_i x) - Q_i Y_1(k_i x)\right). \tag{2.31}$$

On differentiating equation (2.28) with respect to x, the temperature gradient is obtained as

$$\frac{\partial\bar{\Theta}}{\partial x} = \sum_{i=1}^{3} k_i\left[P_i J_1(k_i x) - Q_i Y_1(k_i x)\right]. \tag{2.32}$$

Substituting values of $\bar{e}, \bar{U}, \bar{\phi}, \bar{\Theta}$ from equations (2.28–2.31) in equation (2.25) we get

$$\tau_{xx} = \sum_{i=1}^{3}\left(P_i \left\{ Z_i J_0(k_i x) + \frac{c_0 - 1}{k_i x} R_i J_1(k_i x) \right\} + Q_i \left\{ Z_i Y_0(k_i x) - \frac{c_0 - 1}{k_i x} R_i Y_1(k_i x) \right\} \right), \quad (2.33)$$

$$\tau_{\theta\theta} = \sum_{i=1}^{3}\left(P_i \left\{ Z_i^* J_0(k_i x) - \frac{c_0 - 1}{k_i x} R_i J_1(k_i x) \right\} + Q_i \left\{ Z_i^* Y_0(k_i x) + \frac{c_0 - 1}{k_i x} R_i Y_1(k_i x) \right\} \right), \quad (2.34)$$

where $Z_i = R_i + \bar{b}^* S_i - \bar{\beta}_R,\; Z_i^* = c_0 R_i + \bar{b}^* S_i - \bar{\beta}_R, \quad i = 1, 2, 3.$

2.5 Frequency equations

Substituting the equations (2.29) to (2.33) for thermally insulated boundaries in equation (2.9) and the equations (2.28) to (2.31) and (2.33) for isothermal boundaries in equation (2.10) of transversely isotropic nonlocal thermoelastic cylinder with voids material at inner and outer radii $x = 1$ and $x = \eta$ for LS model of generalized thermoelasticity. On simplifying these equations, we acquire a system of linear equation given below

$$NH = 0, \quad (2.35)$$

where $H = (P_1, P_2, P_3, Q_1, Q_2, Q_3)^T$ and $N = (m_{ij})_{6\times 6};\; i, j = 1 to 6$. Equation (2.35) gives us six algebraic homogeneous linear equations with six unknown parameters. A non-trivial solution has been obtained if and only if coefficient matrix N diminishes which lead to the frequency equation given below:

$$\left| m_{ij} \right| = 0; \quad i, j = 1 \; to \; 6, \quad (2.36)$$

where the parameters m_{ij} ; $i, j = 1 \; to \; 6$ have been defined in thermally insulated/ isothermal conditions in separate cases as follows:

Set I: The elements of m_{ij} ; $i, j = 1 \; to \; 6$ in the frequency equation (2.36) for stress free thermally insulated boundary conditions are

$$\left.\begin{array}{l}
m_{1j} = Z_i J_0(k_i) + \dfrac{c_0 - 1}{k_i} R_i J_1(k_i);\; i, j = 1, 2, 3; \\
m_{1j} = Z_i Y_0(k_i) - \dfrac{c_0 - 1}{k_i} R_i Y_1(k_i), i = 1, 2, 3,\; j = 4, 5, 6 \\
m_{3j} = S_i J_0(k_i); i, j = 1, 2, 3;\; m_{3j} = S_i Y_0(k_i);\; i = 1, 2, 3;\; j = 4, 5, 6; \\
m_{5j} = k_i J_1(k_i); i, j = 1, 2, 3;\; m_{5j} = -k_i Y_{3/2}(k_i); i = 1, 2, 3;\; j = 4, 5, 6;
\end{array}\right\}. \quad (2.37)$$

Set II: The elements of $m_{1j}, m_{2j}, m_{3j}, m_{4j}; j = 1 \ to \ 6$ remains same as in (2.37). The remaining elements of m_{ij} in the frequency equation (2.36) for traction-free isothermal condition are

$$m_{5j} = J_0(k_i);\ i, j = 1,2,3,\ \ m_{5j} = Y_0(k_i);\ i = 1,2,3;\ j = 4,5,6\}. \qquad (2.38)$$

The elements of $m_{2j}, m_{4j}, m_{6j}\ (j = 1 \ to \ 6)$ are obtained by inserting η along with k_i, in the elements of $m_{1j}, m_{3j}, m_{5j}\ (j = 1 \ to \ 6)$.

2.6 Deduction of analytical results

2.6.1 Generalized transversely magneto thermoelastic cylinder with voids

If we ignore non-locality effect i.e. $\zeta_0 = 0$, then the analysis is reduced to generalized transversely isotropic magneto thermoelastic cylinder with voids material.

2.6.2 Classical magneto thermoelastic cylinder

If we establish thermal equilibrium and the nonlocal parameter, voids constants and relaxation time parameter are ignored i.e. $\zeta_0 = 0$, $\alpha = b = M = \xi_1 = \xi_2 = 0$ and $t_0 = 0$ then the analysis of free vibrations has been reduced to the coupled thermoelastic cylinder and the governing equations of the analysis are consistent with Das et al (2013) in the absence of three-phase-lag relaxation time parameters.

2.6.3 Generalized thermoelastic LS model transversely isotropic cylinder

If again the nonlocal parameter, magnetic field constants and voids constants are ignored i.e. $\zeta_0 = 0$, $\mu_e = H_0 = 0$ and $\alpha = b = M = \xi_1 = \xi_2 = 0$, then the analysis has been reduced transversely isotropic thermoelastic hollow cylinder whose governing equations and free vibration analysis are consistent with Sharma et al (2014) in the absence of functionally graded materials.

2.6.4 Elastic cylinder

If the constants i.e. nonlocal, voids, magneto, relaxation times and thermo-mechanical are removed i.e. $\zeta_0 = 0$, $\alpha = b = M = \xi_1 = \xi_2 = 0$, $\mu_e = H_0 = 0$, $t_0 = 0$ and $\beta_R = \varepsilon_T = 0$, then the analysis has been reduced to transversely isotropic elastic cylinder which completely agree with Kele and Tutuncu (2011) in the absence of functionally graded materials.

2.7 Numerical results and discussion

Some numerical simulations and computations have been proposed for the authentication of analytical results in transversely isotropic nonlocal magneto-thermoelastic hollow cylinder with voids material. The numerical results have been performed for generalized thermoelasticity (GTE), coupled thermoelasticity (CTE) and elasticity (E) in the absence and presence of magnetic fields for nonlocal and local thermoelastic hollow cylinder by taking ratio of outer to inner radius $\eta = 1.5,\ 2.0$. Mathematical modeling has been prepared for the transversely isotropic magneto-thermoelastic solid with voids material single crystal of zinc whose physical constant values are given in SI units (Chadwick and Seet (1970))

$$c_{11} = 1.628 \times 10^{11}\, Nm^{-2},\quad c_{12} = 1.562 \times 10^{11}\, Nm^{-2},\ \beta_r = \beta_\theta = 5.75 \times 10^{6}\, Nm^{-2}\ \deg^{-1},$$
$$K = 1.24 \times 10^{2} Wm^{-1} \deg^{-1},\ C_e = 3.9 \times 10^{2}\, JKg^{-1} \deg^{-1},\ \rho = 7.14 \times 10^{3} Kg\, m^{-3},$$
$$T_0 = 296K,\ \tau_0 = 0.05,\ \omega = 10$$

And voids parameters are:

$$\chi = 1.753 \times 10^{-15} m^2,\ \alpha = 3.688 \times 10^{-5} N,\ M = 2.0 \times 10^{6} Nm^{-2} \deg^{-2},$$
$$\xi_1 = \xi_2 = 1.475 \times 10^{10}\, Nm^{-2},\ b = 1.13849 \times 10^{10}\, Nm^{-2}$$

The magnetic field parameters have been assumed as $\mu_e = 4\pi \times 10^{-7} H/m$, $H_0 = 10^8\, A/m$ from Othman and Hilal (2017). The value of nonlocal parameter has been calculated as $\xi_0 = 2.3102$ from Bachher and Sarkar (2019). The secular dispersion relations have been acquired from assumed boundary conditions, which are generally compound transcendental equations, give us the values in the form of complex numbers (real as well as imaginary parts) due to the occurrence of dissipative term in heat conduction equation (2.7). The simulations have been applied to equation (2.36) for the cases of thermally insulated boundary conditions in correct to five decimal places.

The functional numerical Iteration technique has been applied to evaluate the roots of equation (2.36), which is of the type $f(\Omega)=0$. The substitution of $\Omega=\Phi(\Omega)$ is required so that the sequence (Ω_n) of iterations has been generated for essential accuracy level. Here, if Ω_0 has been assumed the initial approximation of the root, then we have $\Omega_1=\Phi(\Omega_0)$, $\Omega_2=\Phi(\Omega_1)$, $\Omega_3=\Phi(\Omega_2)$ and so on and generally we obtain $\Omega_{n+1}=\Phi(\Omega_n);\ n=1,2,3,...$ as reported in Sharma and Walia (2007). The required condition $|\Phi'(\Omega)|<1$ for all $\Omega\in I$, then the approximations will be convergent to the actual value $\Omega=\Omega_a$ of the root, provided $\Omega_0\in I$, here I is assumed interval of the root as expected. The condition for numerical convergence i.e. $|\Omega_{n+1}-\Omega_n|<\varepsilon$, where ε has been chosen small arbitrary number selected randomly to accomplish the required level of accuracy, which might be satisfied. Therefore, the above process is repeated continuously for the values of the frequency parameter Ω (real as well as imaginary part) many times until we obtain desired accuracy level. The numerically analyzed complex values (frequencies) of Ω might be written as $\Omega^m=\Omega_R^m+i\Omega_I^m$. The real part and imaginary part has been considered as natural frequencies $\Omega_R^m=\Omega_R$ and dissipation factor $\Omega_I^m=\Omega_I$ respectively. The value of m is assumed as mode number, corresponds to the root of the equation. The numerically simulated natural frequencies have been presented graphically for theories of GTE, CTE and E thermoelasticity for nonlocal/local thermoelastic hollow cylinder in presence and absence of magnetic field. The real part of the root of frequency equation is denoted as natural frequencies (Ω_R). The natural frequencies (Ω_R) against mode number (m) for nonlocal/local elastic cylinder at outer to inner radius ratio $\eta=1.5$ have been shown graphically in Figs. 2.2(a, b) to Figs. 2.3(a, b) for different models of generalized thermoelastic cylinder with voids in presence and absence of magnetic field. Here 2.3(a) represent vibrations with magnetic field and 2.3(b) represent vibrations without magnetic field. It has been inferred from Fig. 2.2 (nonlocal elastic material) and Fig. 2.3 (local elastic material) that the variation of vibrations are low initially and with increasing values of m, the variation of vibrations go on increasing. On removing nonlocal, voids and magnetic field parameters from the governing equations and field functions, therefore, frequency equations (2.35) and (2.36) have been modified accordingly and presented for natural frequencies versus mode number in Fig. 2.3(c). The variation of natural frequency vibrations go on increasing with increasing mode number. The behavior of natural frequency vibrations in the Fig. 2.3(c) has similar variation with the qualitative nature of earlier published manuscript Sharma (2020a). The behavior of vibrations is lower in the presence of magnetic field in contrast to the absence of magnetic field for nonlocal and local elastic materials. The roots of frequency equation might be presented in real and imaginary parts which have been assumed as quality factor related to thermoelastic damping. The fractions of lost energy per cycle of vibrations, has been calculated from Moosapour et al. (2014) as

$$Q = \frac{\left(\mathrm{Re}(\Omega_R^m)^2 + \mathrm{Im}(\Omega_I^m)^2\right)^{\frac{1}{2}}}{2\left|\mathrm{Im}(\Omega_I^m)\right|}.$$

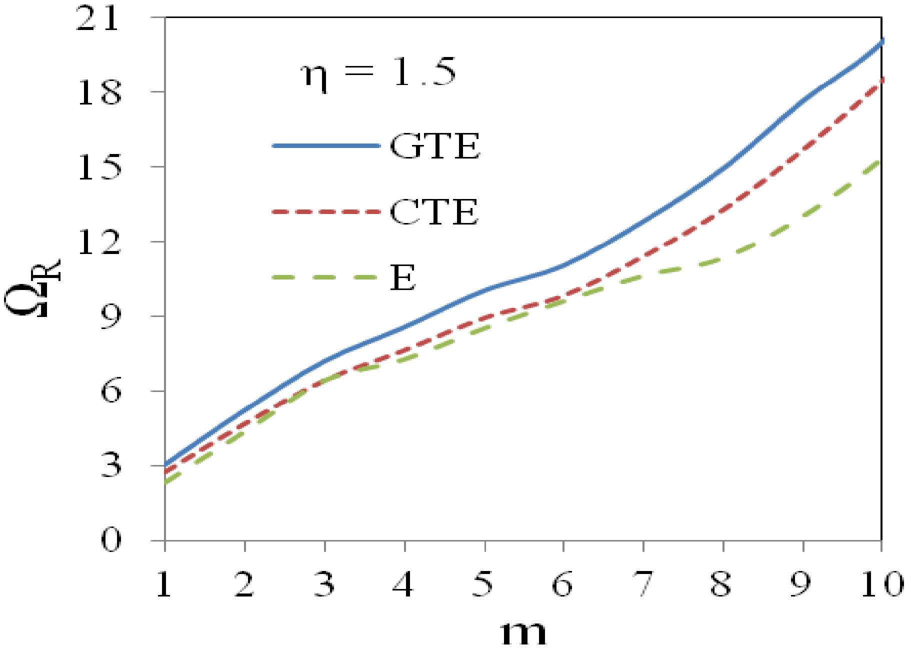

Figure 2.2(a): Natural frequencies (Ω_R) versus mode number (m) for different models of thermoelasticity at $\eta = 1.5$ in nonlocal elastic cylinder with voids with magnetic field.

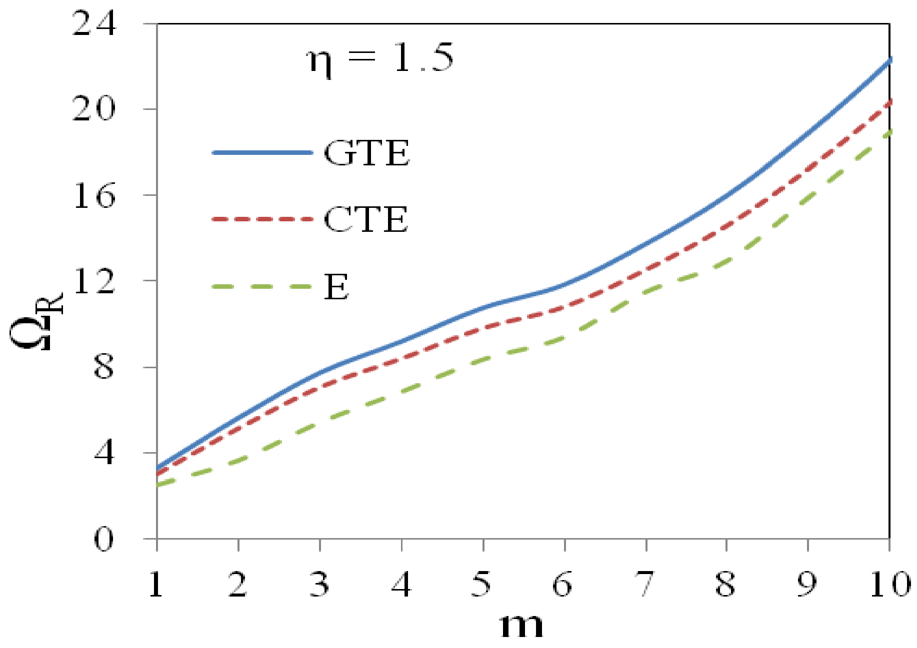

Figure 2.2(b): Natural frequencies (Ω_R) versus mode number (m) for different models of thermoelasticity at $\eta = 1.5$ in nonlocal elastic cylinder with voids without magnetic field.

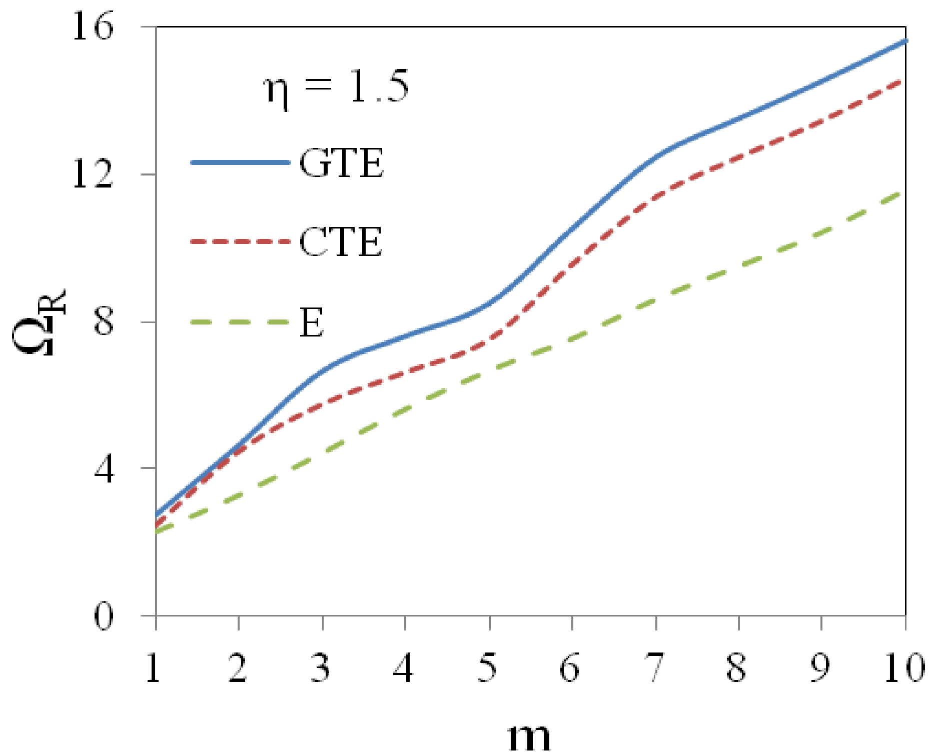

Figure 2.3(a): Natural frequencies (Ω_R) versus mode number (m) for different models of thermoelasticity at $\eta = 1.5$ in local elastic cylinder with voids and magnetic field.

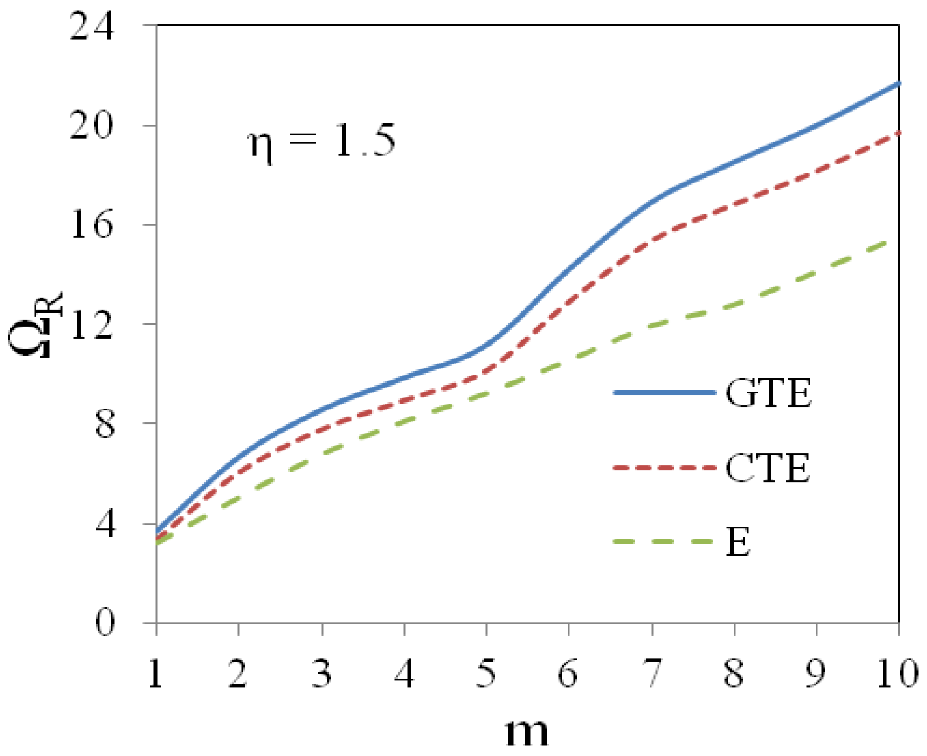

Figure 2.3(b): Natural frequencies (Ω_R) versus mode number (m) for different models of thermoelasticity at $\eta = 1.5$ in local elastic cylinder with voids and without magnetic field.

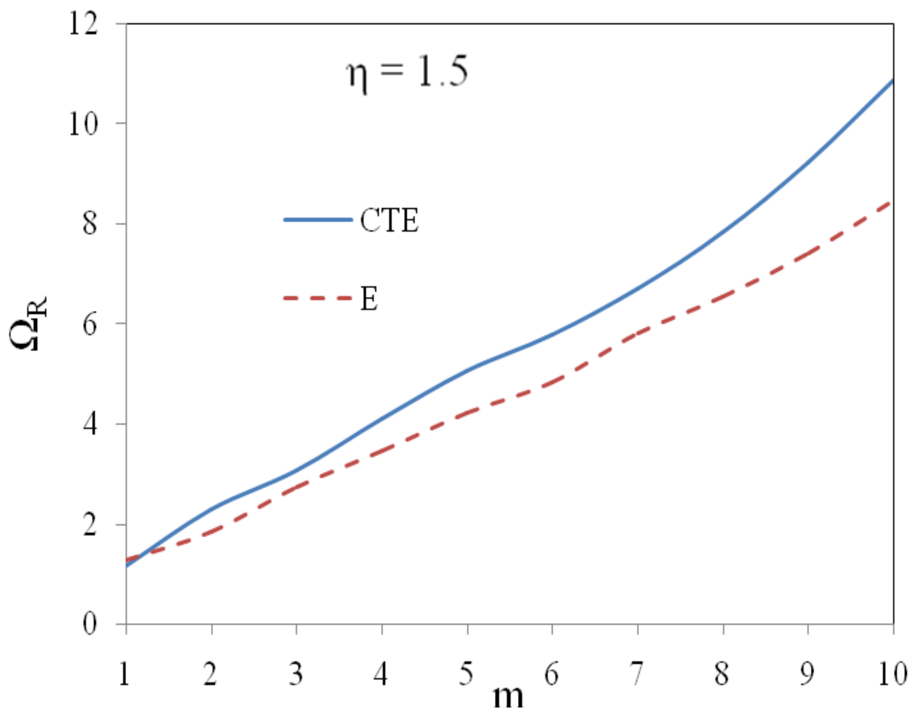

Figure 2.3(c): Natural frequencies (Ω_R) versus mode number (m) for different models of thermoelasticity at $\eta = 1.5$ in local elastic cylinder without nonlocality, viods and magnetic field.

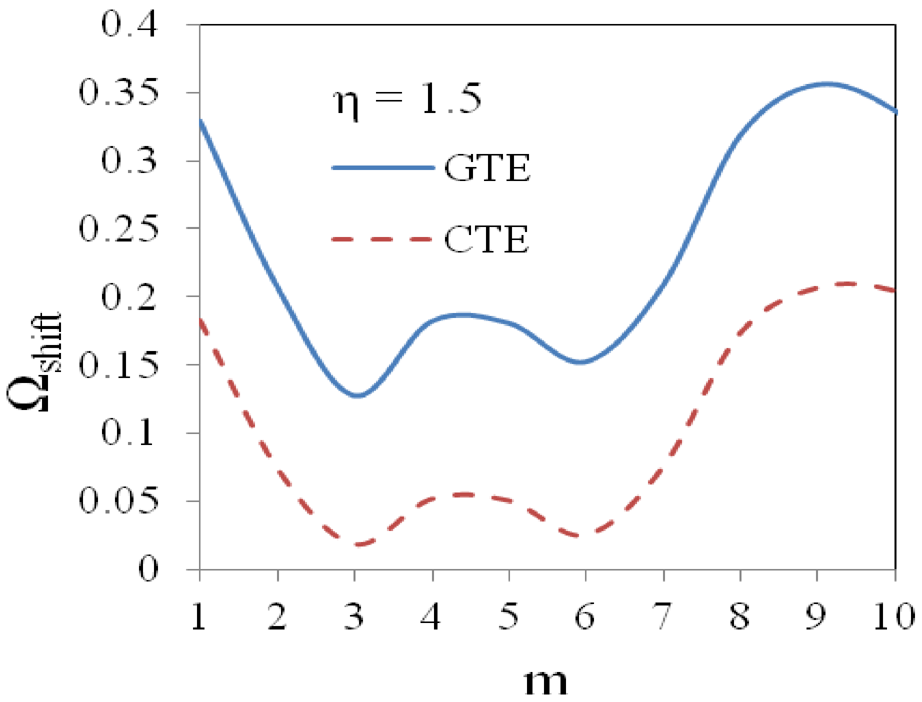

Figure 2.4(a): Frequency shift (Ω_{Shift}) versus mode number (m) for different models of thermoelasticity at $\eta = 1.5$ in nonlocal elastic cylinder with voids with magnetic field.

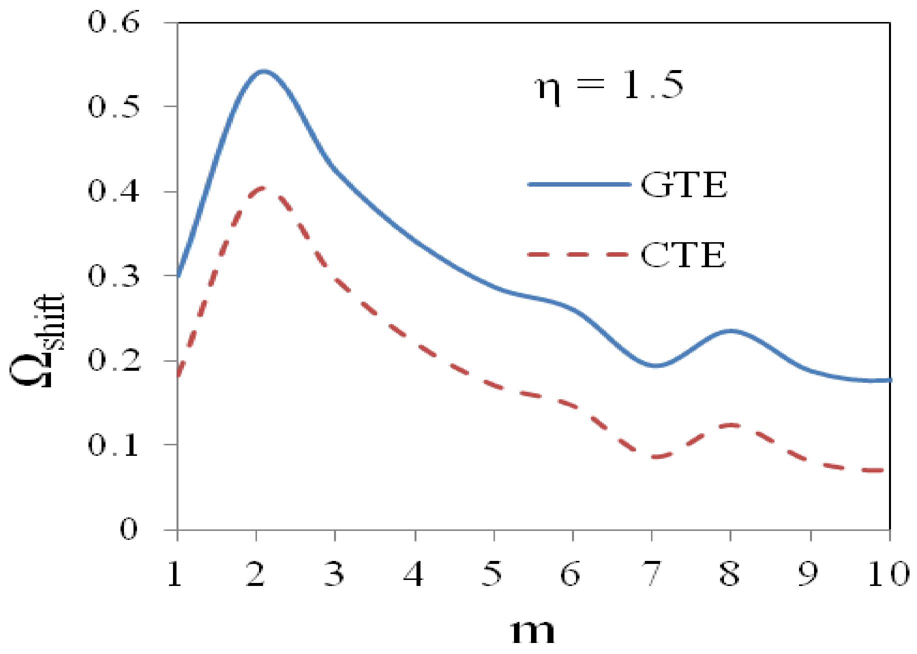

Figure 2.4(b): Frequency shift (Ω_{Shift}) versus mode number (m) for different models of thermoelasticity at $\eta = 1.5$ in nonlocal elastic cylinder with voids and without magnetic field.

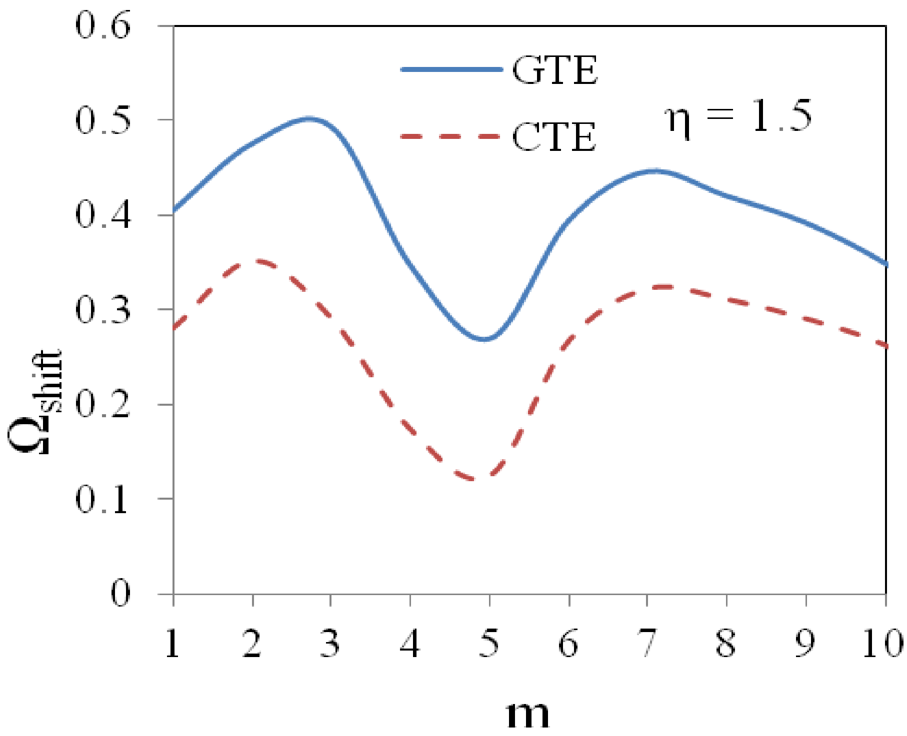

Figure 2.5(a): Frequency shift (Ω_{Shift}) versus mode number (m) for different models of thermoelasticity at $\eta = 1.5$ in local elastic cylinder with voids with magnetic field.

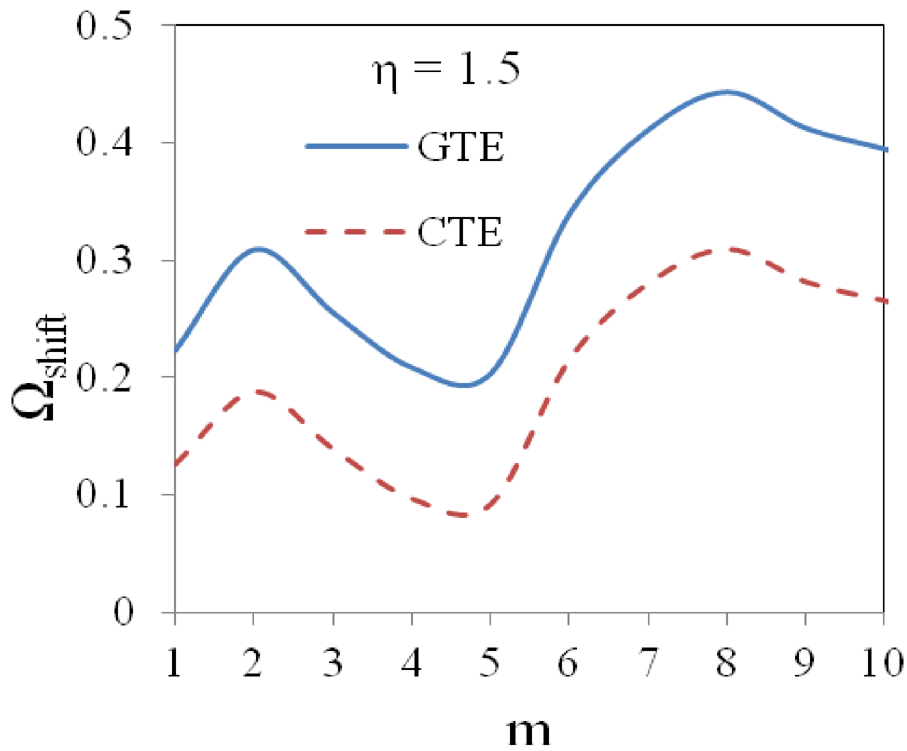

Figure 2.5(b): Frequency shift (Ω_{Shift}) versus mode number (m) for different models of thermoelasticity at $\eta = 1.5$ in local elastic cylinder with voids and without magnetic field.

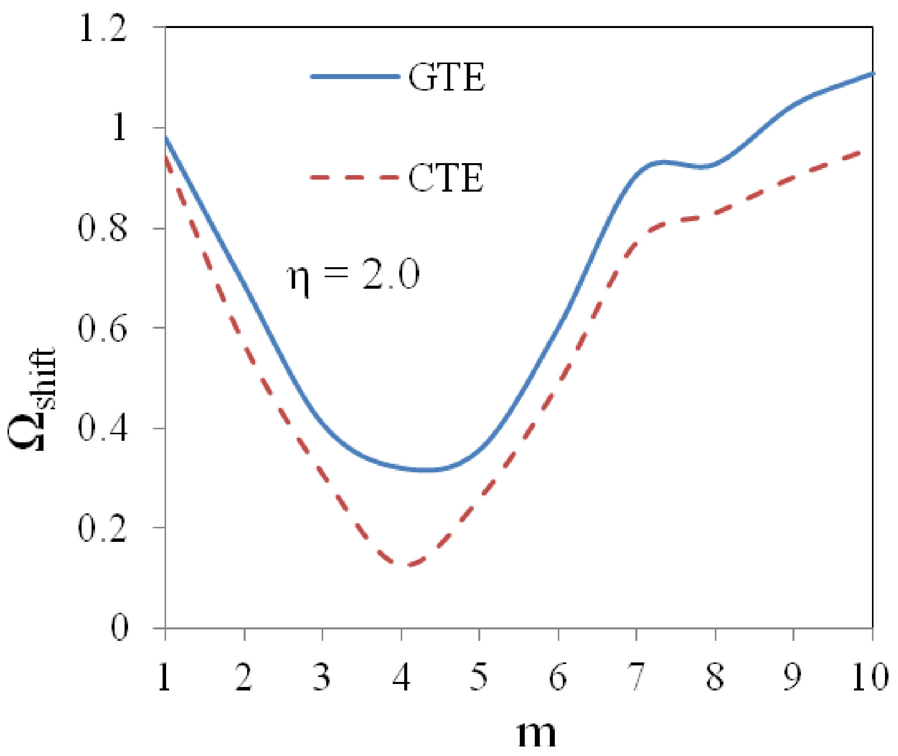

Figure 2.6(a): Frequency shift (Ω_{Shift}) versus mode number (m) for different models of thermoelasticity at $\eta = 2.0$ in nonlocal elastic cylinder with voids with magnetic field.

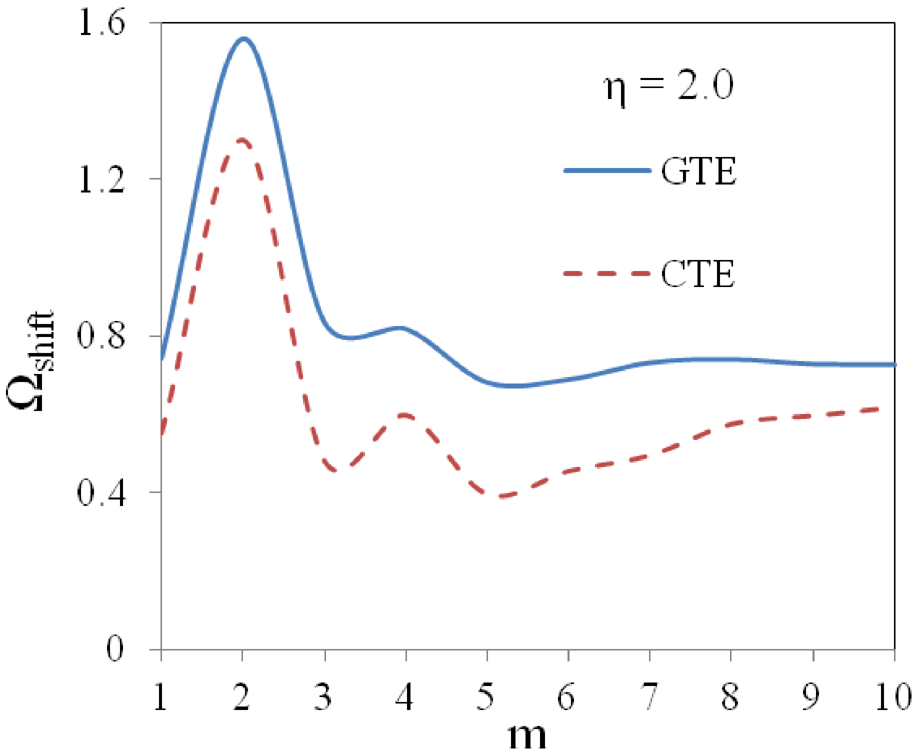

Figure 2.6(b): Frequency shift (Ω_{Shift}) versus mode number (m) for different models of thermoelasticity at $\eta = 2.0$ in nonlocal elastic cylinder with voids without magnetic field.

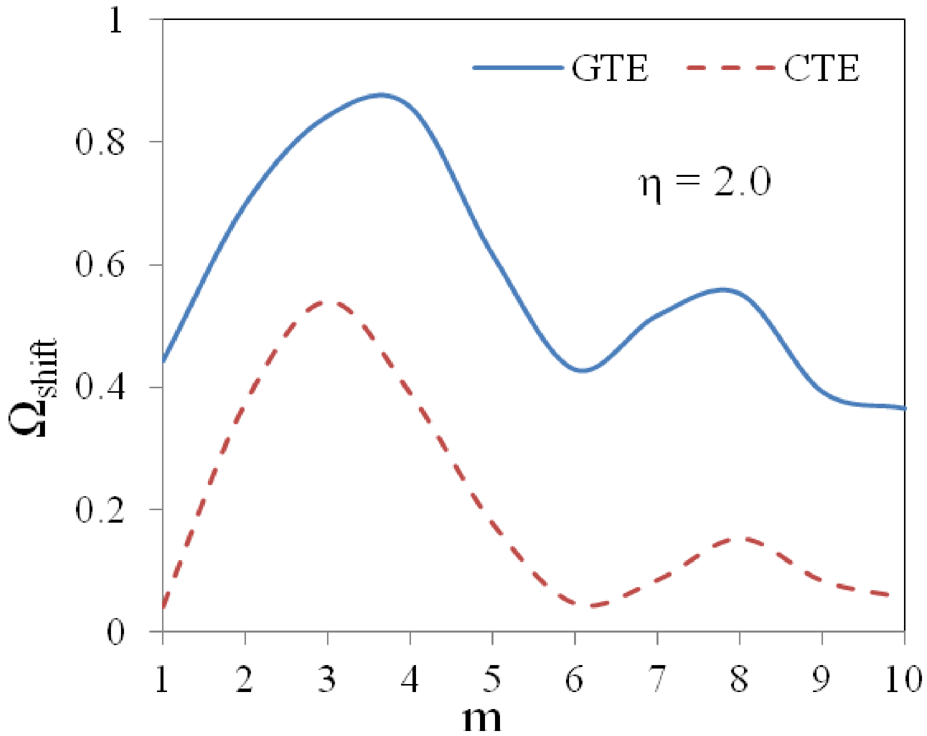

Figure 2.7(a): Frequency shift (Ω_{Shift}) versus mode number (m) for different models of thermoelasticity at $\eta = 2.0$ in local elastic cylinder with voids with magnetic field

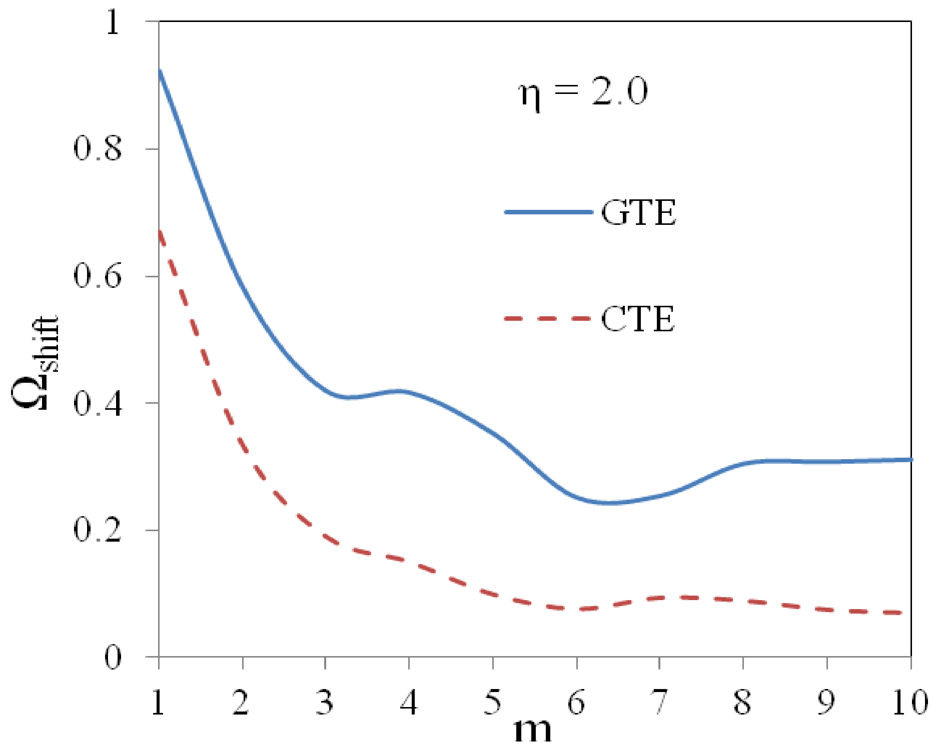

Figure 2.7(b): Frequency shift (Ω_{Shift}) versus mode number (m) for different models of thermoelasticity at $\eta = 2.0$ in local elastic cylinder with voids without magnetic field.

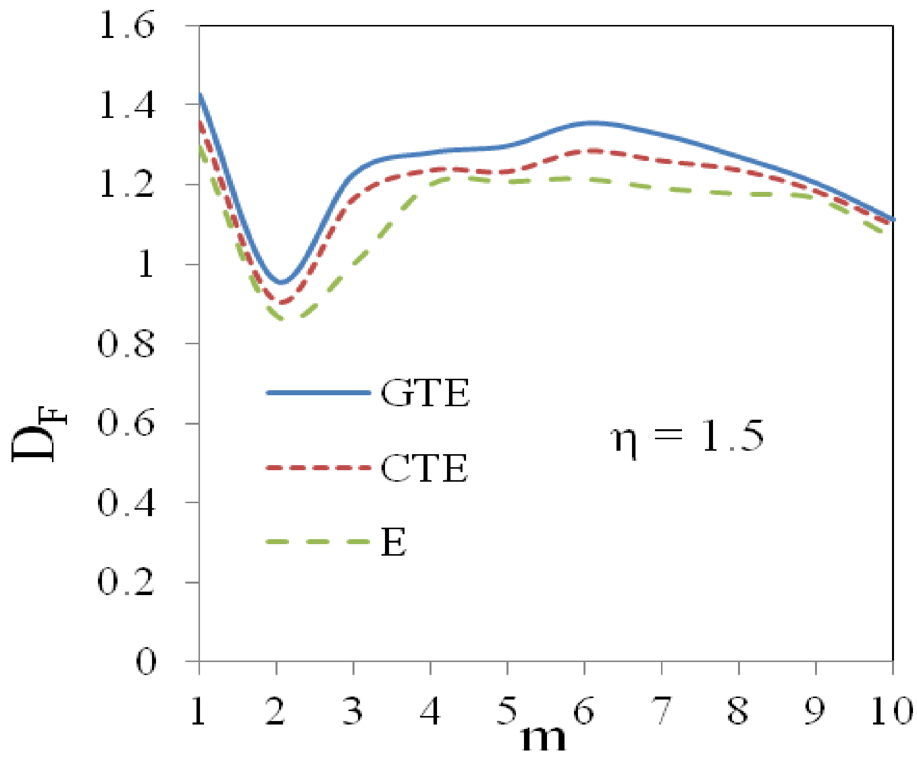

Figure 2.8(a): Thermoelastic damping (D_F) versus mode number (m) for different models of thermoelasticity at $\eta = 1.5$ in nonlocal elastic cylinder with voids with magnetic field.

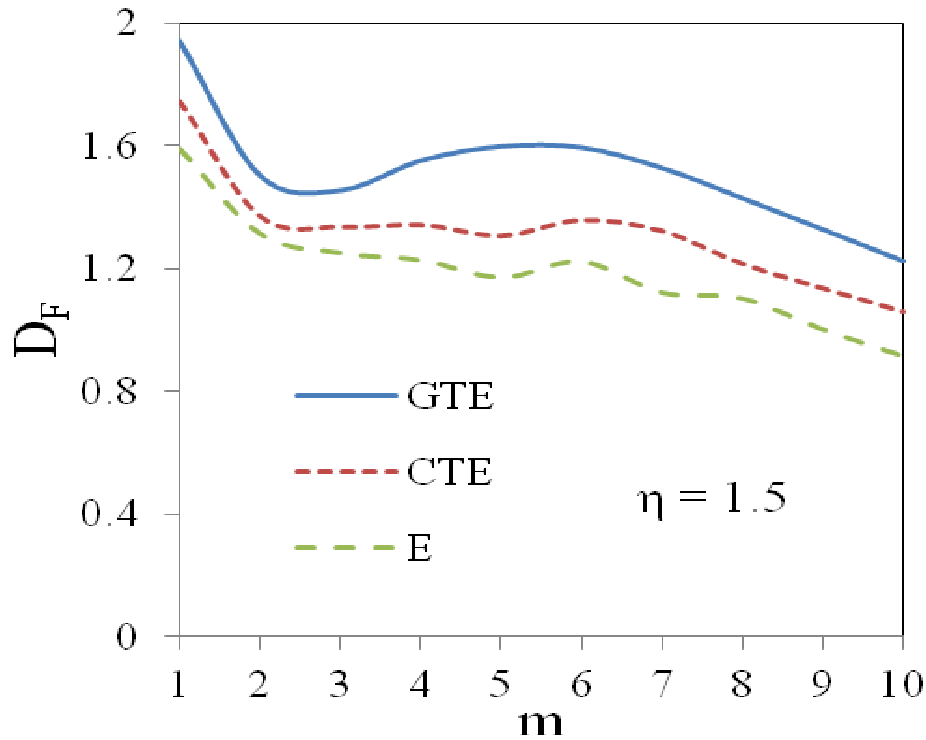

Figure 2.8(b): Thermoelastic damping (D_F) versus mode number (m) for different models of thermoelasticity at $\eta = 1.5$ in nonlocal elastic cylinder with voids without magnetic field.

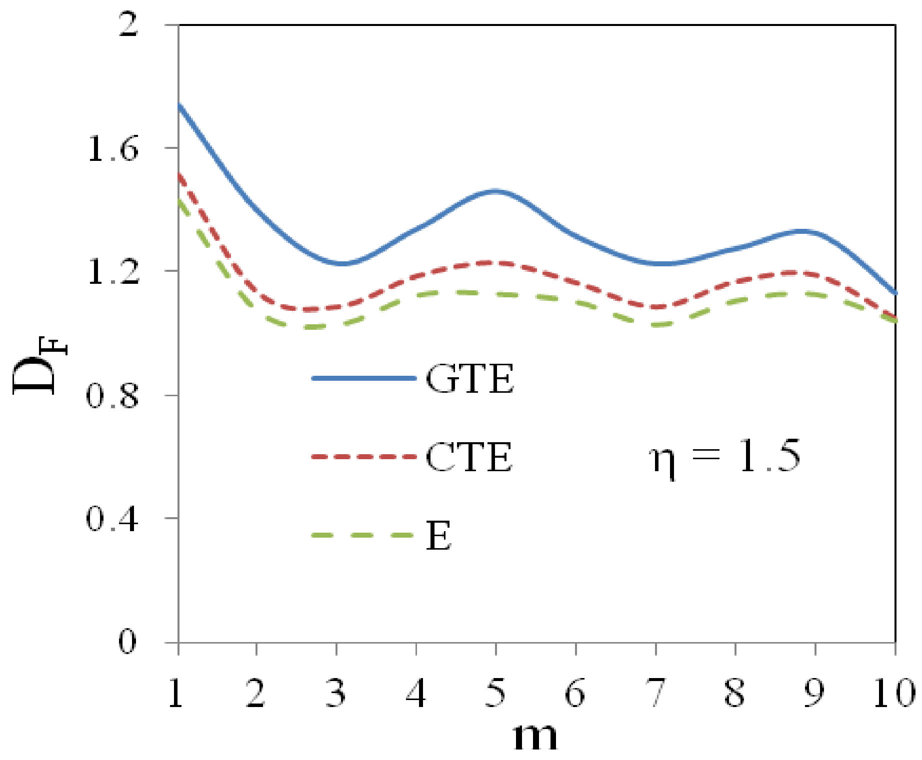

Figure 2.9(a): Thermoelastic damping (D_F) versus mode number (m) for different models of thermoelasticity at $\eta = 1.5$ in local elastic cylinder with voids with magnetic field.

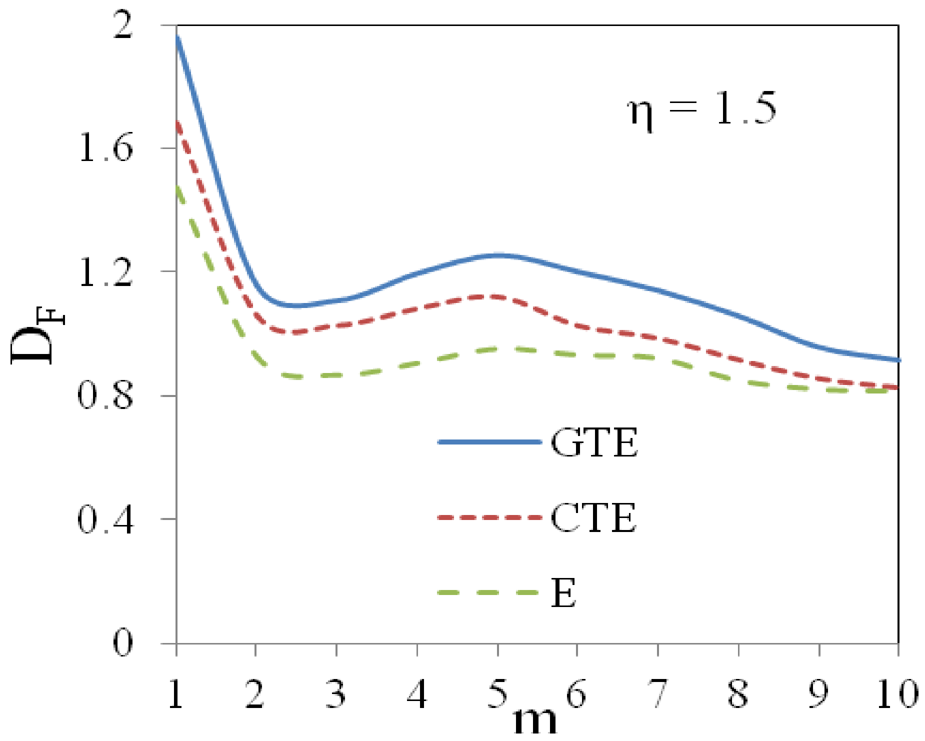

Figure 2.9(b): Thermoelastic damping (D_F) versus mode number (m) for different models of thermoelasticity at $\eta = 1.5$ in local elastic cylinder with voids without magnetic field.

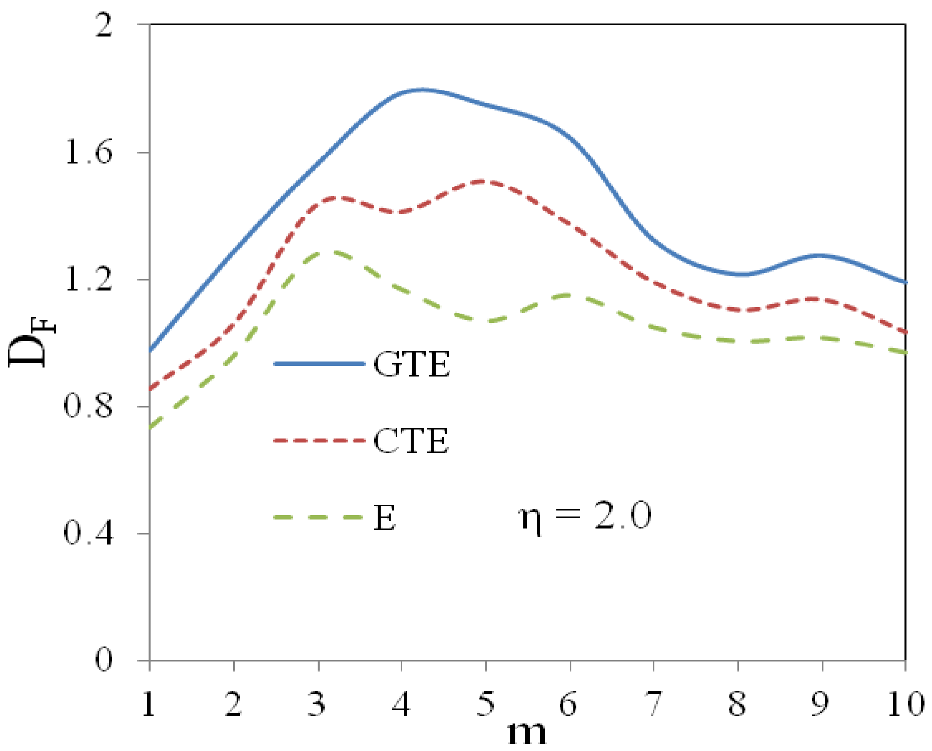

Figure 2.10(a): Thermoelastic damping (D_F) versus mode number (m) for different models of thermoelasticity at $\eta = 2.0$ in nonlocal elastic cylinder with voids with magnetic field.

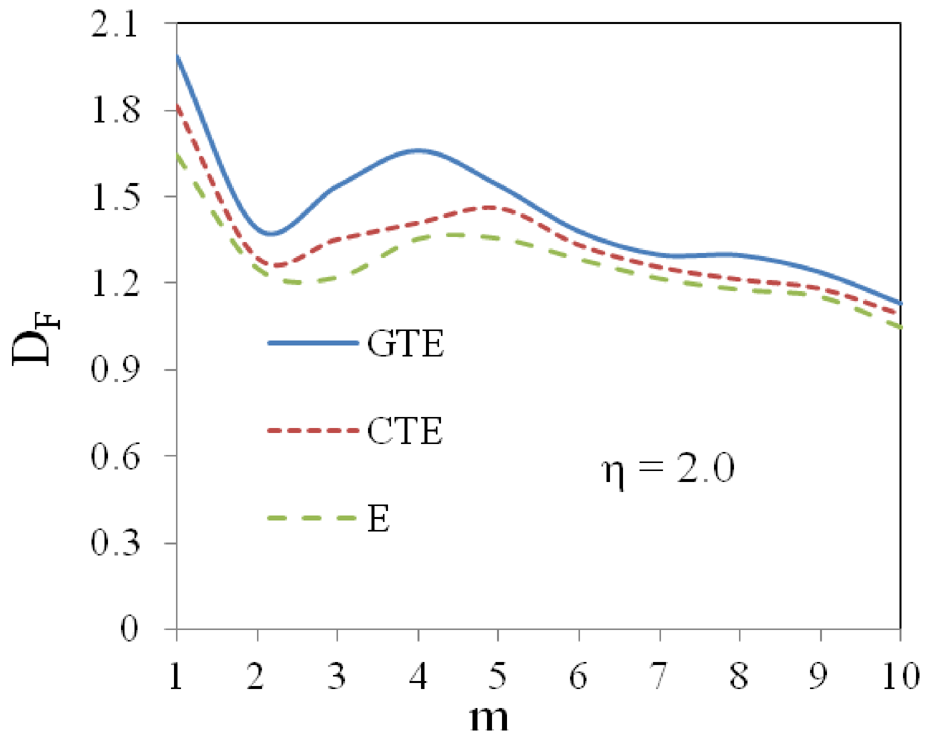

Figure 2.10(b): Thermoelastic damping (D_F) versus mode number (m) for different models of thermoelasticity at $\eta = 2.0$ in nonlocal elastic cylinder with voids without magnetic field.

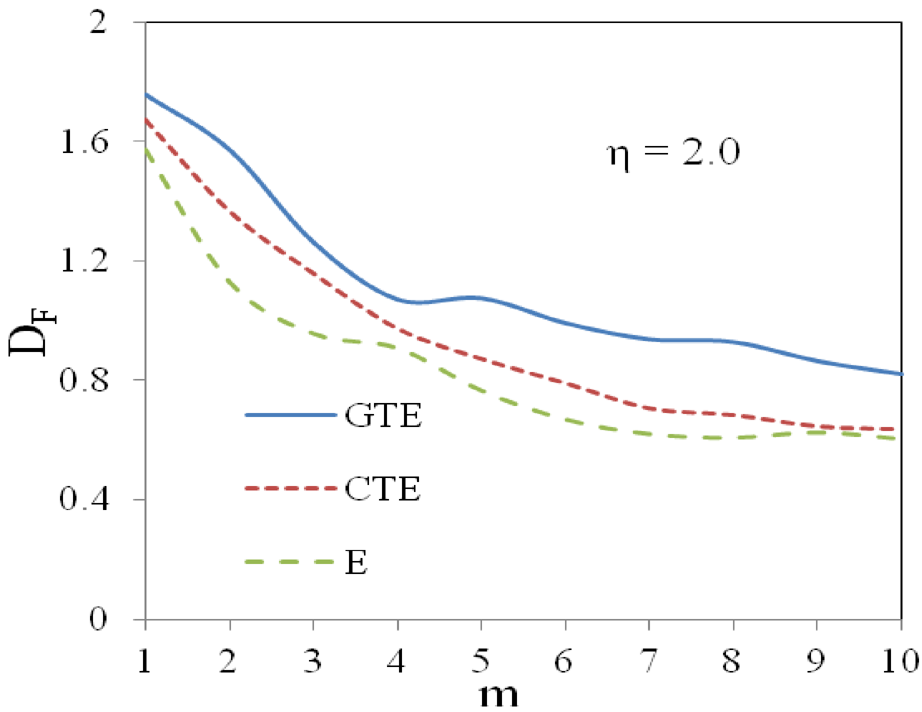

Figure 2.11(a): Thermoelastic damping (D_F) versus mode number (m) for different models of thermoelasticity at $\eta = 2.0$ in transversely isotropic local elastic cylinder with voids with magnetic field.

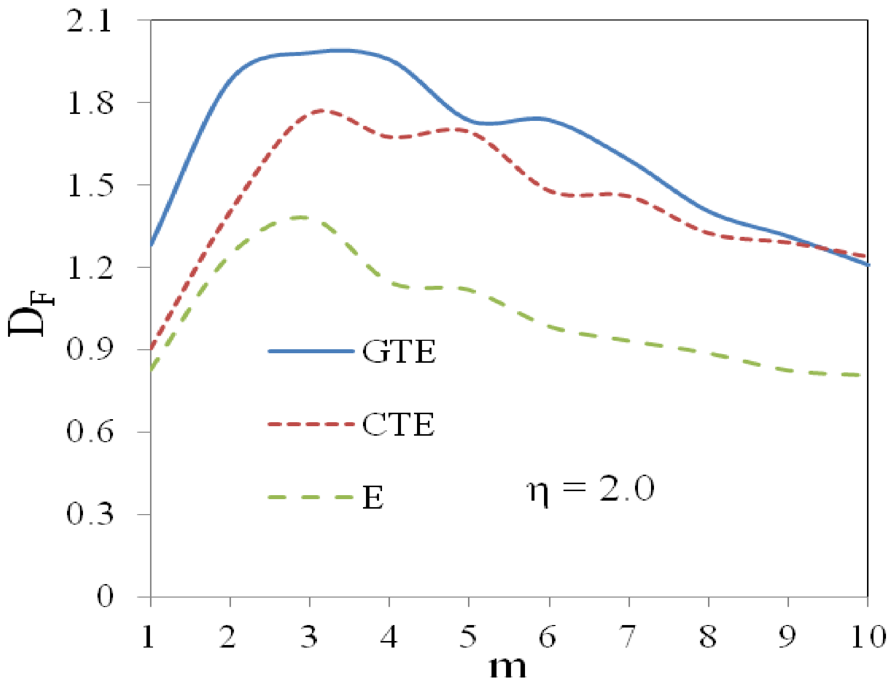

Figure 2.11(b): Thermoelastic damping (D_F) versus mode number (m) for different models of thermoelasticity at $\eta = 2.0$ in transversely isotropic local elastic cylinder with voids without magnetic field.

The value of denominator multiple with 2 arises because of the generated mechanical energy of nonlocal elastic hollow cylinder with voids material is relative to real part. This has been observed from computations that frequencies with imaginary part are less in comparison with real part. Therefore thermoelastic damping (inverse quality factor) (Q^{-1}) for the cases of GTE, CTE and E has been obtained from Sharma et al. (2014) as $Q^{-1} = 2\left|\frac{\Omega_I}{\Omega_R}\right|$. Here thermoelastic damping Q^{-1} has been denoted as D_F . The fractional error obtained from Iterative computation is $\varepsilon^{(Z^K)}$ in the real part of frequency Ω_R^m is defined as $\varepsilon^{(Z^K)} = \left(\mathrm{Re}(\Omega_R^m)^k - \mathrm{Re}(\Omega_R^m)^{k-1}\right)/\,\mathrm{Re}(\Omega_R^m)^{k-1}$ (Moosapour et al. (2014)). Therefore the error $\varepsilon^{(Z^*)}$ will go down below the accepted value and the process of iteration ends. Hence the frequency shift (Ω_{shift}) of nonlocal generalized transversely isotropic thermoelastic hollow cylinder with voids material is defined as $\Omega_{shift} = \left|\frac{(\Omega_R^{Z^*} - \Omega_R^E)}{\Omega_R^E}\right|$ (Sharma et al. (2014)). Here Z^* stands for generalized thermoelasticty (GTE), coupled thermoelasticity (CTE) and elasticity (E). Fig. 2.4 has been presented for frequency shift (Ω_{shift}) versus mode number (m) for different models of thermoelasticity at normalized thickness $\eta = 1.5$ for nonlocal elastic cylinder with voids in presence and absence of magnetic field. It is observed from Fig. 2.4(a) that initially the variation of frequency shift vibrations are larger, as we move from left to right, the behavior of vibrations dip between $3.0 \le m \le 6.0$, and go on increasing to become linear at $m = 9.0$. Fig. 2.4(b) depicts that the variation of frequency shift vibrations is initially low, achieve peak value at $m = 2.0$ and as the value of m increases, the variation of vibrations go on decreasing. The Fig. 2.5 has been represented for frequency shift (Ω_{shift}) versus mode number (m) for the models of thermoelasticity i.e. GTE, CTE and E at normalized thickness $\eta = 1.5$ for local elastic cylinder with voids in presence and absence of magnetic field. It is observed from Figs. 2.5(a) and 2.5(b) that initially the frequency shift is low, increases up to $m = 2.0$, dip at $m = 5.0$, after achieving its magnitude to extreme value, it decreases linearly. This has to be noticed from Figs. 2.4 and 2.5 that the variation of frequency shift vibrations is larger in case of GTE in contrast to CTE and E. Fig. 2.6 and 2.7 have been shown for frequency shift (Ω_{shift}) versus mode number (m) for the generalized thermoelastic models i.e. GTE, CTE and E at normalized thickness $\eta = 2.0$ for nonlocal/local elastic cylinders with voids in presence/absence of magnetic field. Fig. 2.6(a) depicts that the variations are larger initially, with increasing values of mode number, the variations decreases up to $m = 4.0$, increases till $m = 8.0$, after that its behavior is noticed to be linear. It is observed from Fig. 2.6(b) that the variation of frequency shift vibrations is initially low, achieve peak value at $m = 2.0$ and as we move from left to right the vibrations become linear at $m = 5.0$. The Fig. 2.7(a) tells that the variation of frequency shift vibrations are low initially, achieve peak value at $m = 3.0$, and with increasing values of mode number the behavior of vibrations decreases to become linear at $m = 9.0$. It has been revealed from Fig. 2.7(b) that the behavior of vibrations are larger initially, as value of mode number increases the vibrations go on decreasing and become linear at $m = 6.0$.

Thermoelastic damping (D_F) versus mode number (m) has been represented in Figs. 2.8 and 2.9 for the generalized thermoelastic models i.e. GTE, CTE and E at normalized thickness $\eta = 1.5$ for nonlocal and local elastic cylinders with voids in presence/absence of magnetic field. It is observed from Fig. 2.8 that in both the cases i.e. with and without magnetic field the variations are larger initially and with increasing value of mode number, the variation of thermoelastic damping vibrations dip at $m = 2.0$ increases slightly to become linear. The Fig. 2.9 which has been presented for local case depicts that initially vibrations are larger, decreases up to $m = 3.0$ and then becomes linear with increasing values of m . The thermoelastic damping (D_F) versus mode number (m) for different models of thermoelasticity i.e. GTE, CTE and E at normalized thickness $\eta = 2.0$ for nonlocal/local elastic cylinders with voids in presence/absence of magnetic field have been presented in Figs. 2.10 and 2.11. Fig. 2.10(a) reveals that initially variation of thermoelastic damping vibrations are low, achieve maximum amplitude between $3.0 \le m \le 5.0$, then decreases linearly as we move from left to fight. It is to be noted from Fig. 2.10(b) that the variations are larger initially and with an increase in the value of mode number the variation of thermoelastic damping achieve its magnitude, then keep on decreasing linearly. It has been revealed from Fig. 2.11(a) that initially the variations of thermoelastic damping vibrations are larger, and with increasing values of mode number, the vibrations go on decreasing. It is to be noticed from 2.11(b) that initially thermoelastic damping vibrations are low, achieve maximum amplitude between $2.0 \le m \le 4.0$ and with an increase in the value of mode number the vibrations go on decreasing. This has been observed from all the figures that the vibrations are larger in case of GTE in comparison with CTE and elasticity cases. Also due to the effect of magnetic field the behavior of vibrations are lower in presence of magnetic field in contrast to absence of magnetic field. The behavior of thermoelastic damping is found to increase and decrease with increasing value of mode number due to coupling of elastic field between mechanical, thermal, voids and magnetic fields.

2.8 Conclusions

The free vibrations of electro-magneto transversely isotropic nonlocal thermoelastic hollow cylinder with voids material are investigated. With the help of time harmonics the governing partial differential equations are resolved into ordinary differential equations by applying time harmonics. The outer and inner surfaces of hollow cylinder have been considered stress free and thermally insulated/isothermal. From the calculated analytical and numerical results/discussions, following conclusions have been observed:

1. The analytical results for derived frequency equations have been examined computationally.
2. The numerical results for the effect of LS model of generalized magneto thermoelastic hollow cylinder have been shown for the field functions such as thermoelastic damping and frequency shift with and without magnetic field.
3. The effect of magnetic field clearly indicates that the behavior of vibrations is larger in absence of magnetic field in contrast to presence of magnetic field.
4. It has been concluded from all the figures that in case of GTE model the vibrations are larger in contrast to CTE and E cases due to effect of relaxation time parameters.
5. The natural frequency graphs clearly indicate that with increasing values of mode number, the behavior of vibrations keeps increasing.
6. In observing the behavior of figures, it is observed that after getting maximum and minimum amplitudes of variations, the behavior of thermoelastic damping becomes linear because of coupling between elastic and thermal fields.
7. It is noticed that the field functions of free vibrations have been influenced by non-locality effect and represented for local and nonlocal cases with and without magnetic fields.

8. The study might find engineering applications in industry and defense that the theories of thermoelasticity i.e. LS and CTE models provide better and easier description to allow voids, diffusion and relaxation, where the process of relaxation times are comparable.

9. From the results of the study, researchers receive the motivation to inspect the free vibration analysis of conducting elastic, thermoelastic and magneto-thermoelastic material with voids as novel applications in continuum mechanics.

10. The chapter might prove useful applications for those who are working in the field of seismology for drilling and mining in the earth's crust. The study also find applications that physicist who are working in field of designing of new materials, for researchers in free vibrations in material science, designers of new materials as well as in practical situations as in geomagnetic, optics, geophysics, acoustics, and oil prospecting etc.